Future Prospects of Spent Coffee Ground Valorisation Using a Biorefinery Approach

Lyn Yeoh[a,b], Kok Siew Ng[a*]

[a] Department of Engineering Science, University of Oxford, Parks Road, Oxford OX1 3PJ, United Kingdom.

[b] Christ Church, University of Oxford, St Aldates, Oxford OX1 1DP, United Kingdom.

Abstract

In the UK, half a million tonnes of spent coffee ground (SCG) waste are generated annually. Current SCG management practices of landfill and energy-from-waste (EfW) facilities either underutilise its valuable constituents or have negative environmental impacts. This study investigates the prospects of SCG-based biorefineries by assessing the impact of biorefinery size, location and products on economic and environmental performances. Two biorefinery design configurations are proposed. Configuration I produces biodiesel and electricity whilst Configuration II produces biodiesel and high-value chemicals. From these configurations, four biorefinery scenarios are analysed at a 10% discount rate with 2019 as the reference year. Configuration I using SCG from London coffee establishments yields a negative net present value (*NPV*) of −£3.9 million and 22% greater greenhouse gas (GHG) emissions than conventional rapeseed biodiesel production. Changing the SCG source to a coffee factory increases biorefinery size by 2.3 times but still produces a negative *NPV*. Using Configuration II to process SCG from coffee shops significantly improves *NPV*. However, without on-site energy generation, its GHG emissions are greater than those from conventional production methods of the high-value chemicals. An on-site Configuration I using SCG from the coffee factory yields the best performance. It produces a *NPV* of £3.1 million and GHG emissions 85% and 13% lower than that of SCG landfilling and conventional biodiesel. Overall, these findings demonstrate the potential of extracting value from SCG waste using a biorefinery approach, revealing a strong likelihood that future SCG biorefineries will be large scale and on-site of SCG production.

Keywords: Circular economy; spent coffee grounds; biorefinery; biofuels; techno-economic analysis; carbon footprint analysis

*** Corresponding author.** Email: kok.ng@eng.ox.ac.uk (KS Ng)

Nomenclature

AD	Anaerobic digestion
CEPCI	Chemical Engineering Plant Cost Index
EfW	Energy-from-waste
f.o.b	Free on board
FFA	Free fatty acids
GHG	Greenhouse gas
HEN	Heat exchanger network
HMF	Hydroxymethylfurfural
IEA	International Energy Agency
OPEX	Operating expenditure
PHB	Polyhydroxybutyrate
SA	Succinic acid
SCG	Spent coffee ground
CC	Annualised capital cost (£/y)
C_{CARB}	Carbon costs from plant's net CO_2 produced (£/y)
C_f	Cash flow in a particular year (£)
$COST_b$	Equipment cost at base size and base year (£)
$COST_f$	Equipment free on board cost at base year (£)
C_r	Equipment cost at reference year (£)
CR_E	Emissions credit from electricity exported to grid (kg CO_2-eq./t SCG)
CRF	Capital recovery factor
C_{RM}	Cost of raw materials (£/y)
CR_P	Emissions credit from displaced use of conventionally produced products (kg CO_2-eq./t SCG)
C_U	Cost of utilities (£/y)
C_{WT}	Waste treatment costs (£/y)
dr	Discount rate (%)
E_{COMB}	Emissions from combustion of biodiesel product (kg CO_2-eq./t SCG)
E_{ENERGY}	Emissions from energy consumed (kg CO_2-eq./t SCG)

$\boldsymbol{EP}$	Economic potential (£)
$\boldsymbol{E_P}$	Net direct CO_2 emissions of plant (kg CO_2-eq./t SCG)
$\boldsymbol{E_{RM}}$	Emissions from raw materials used (kg CO_2-eq./t SCG)
$\boldsymbol{E_{TRAN}}$	Emissions from SCG transport (kg CO_2-eq./t SCG)
$\boldsymbol{E_{WT}}$	Emissions from waste treatment (kg CO_2-eq./t SCG)
$\boldsymbol{h}$	Annual number of operating hours (h)
$\boldsymbol{IV}$	CEPCI Index value
$\boldsymbol{N_{equip}}$	Total number of equipment
$\boldsymbol{Np}$	Total number of products
$\boldsymbol{NPV}$	Net present value (£)
$\boldsymbol{OC}$	Annual operating cost (£/y)
$\boldsymbol{p}$	Base unit price of product (£/kg)
$\boldsymbol{PL}$	Plant production lifetime (y)
$\boldsymbol{r}$	Hourly production rate (kg/h)
$\boldsymbol{R}$	Scaling exponent
$\boldsymbol{SIZE_b}$	Equipment base size (units depend on equipment type)
$\boldsymbol{SIZE_f}$	Equipment current size (units depend on equipment type)
$\boldsymbol{TCC}$	Total capital cost (£)
$\boldsymbol{VAR}$	Annual variable operating costs (£/y)
$\boldsymbol{\Delta T_{min}}$	Minimum temperature difference (˚C)
$\boldsymbol{\Delta\%}$	Percentage change in product price (%)

1 Introduction

Coffee is one of the world's most popular beverages. With a global daily consumption of 2.25 billion cups, its beans are second only to petroleum as an internationally traded commodity (Giller et al., 2017). Coffee consumption generates large amounts of waste, with the UK alone producing an estimated half a million tonnes of wet spent coffee ground (SCG) annually (Recycling Magazine, 2019). Currently, most SCG produced worldwide are disposed in landfills, where its decomposition releases greenhouse gas (GHG) emissions into the atmosphere and acidic leachate containing ecotoxic compounds (Kookos, 2018; Park et al., 2016). SCG is also treated via energy-from-waste (EfW), which allows for energy recovery (Schmidt et al., 2020) but leaves the rich variety of valuable organic compounds found in SCG severely underutilised. Energy recovery from SCG is

done by a company known as Bio-bean, which processes the waste into pellets or logs to be sold as renewable solid fuel (Bio-bean, 2021).

Insoluble lignocellulosic material (lignin, cellulose and hemicellulose) constitutes almost 70 wt% of dry SCG, while proteins and oils make up 11% and 15%, respectively (Obruca et al., 2015). Most SCG studies considered lignin as a fuel to deliver energy requirements (Mata et al., 2018; Saratale et al., 2020). The only SCG study found to isolate lignin was performed by Lee et al. (2019), utilising the Organosolv pre-treatment. The sugar monomers of SCG cellulose and hemicellulose have been recovered for use in microbial growth and the production of chemicals or materials (Kourmentza et al., 2018). Obruca et al. (2015) and Wang et al. (2010) found that concentrations of fermentable sugars in SCG hydrolysate can be increased through combining dilute acid hydrolysis and enzymatic digestion. Chiyanzy et al. (2015) investigated the application of steam explosion pre-treatment as an effective method to reduce the enzyme dosage required in the ensuing enzymatic hydrolysis of SCG. However, Mayanga-Torres et al. (2017) found that temperature above 150˚C rapidly increases the formation of toxic sugar degradation products such as hydroxymethylfurfural (HMF) and furfural, which inhibit microbial activity in subsequent fermentation processes. Kovalcik et al. (2018) suggested that the removal of toxic co-contaminants present in SCG hydrolysates via detoxification steps may increase utilisation of the waste. Using different microorganism strains, the fermentation of recovered SCG sugars can yield a wide range of products, such as bioethanol, bioplastics and high-value platform chemicals (Kourmentza et al., 2018).

On average, SCG contains around 15% oil (Kondamudi et al., 2008). Synthesis of biodiesel from SCG oil via transesterification has been demonstrated (Al-Hamamre et al., 2012; Kondamudi et al., 2008), where transesterification is the reaction between triglycerides and lower alcohols. These studies used solvent extraction methods to isolate the oil from SCG. To eliminate the need for a separate oil extraction process, the *in-situ* transesterification of SCG has been investigated, where simultaneous extraction and transesterification produced biodiesel (Tuntiwiwattanapun et al., 2017).

However, this procedure has been criticised for its high energy consumption (Kookos, 2018). One of the challenges of SCG oil transesterification arises due to its high free fatty acid (FFA) content, which reacts with alkali catalysts to form soap (Tuntiwiwattanapun et al., 2017). To avoid significant soap formation and the deactivation of the alkaline catalyst in transesterification, the SCG must be of less than 3 wt% FFA (Trejo-Zárraga et al., 2018). To address this, Caetano et al. (2014) performed acid esterification and alkaline transesterification on SCG oil, resulting in a 37% increase in biodiesel yields when compared against the direct transesterification of SCG. Typical yields of biodiesel from esterification and transesterification have been found to be around 0.84 kg biodiesel/kg oil (Abdelaziz et al., 2020, 2019). Energy recovery from SCG has been explored extensively in literature. Various studies showed that dried SCG has a lower heating value (18.8 MJ/kg at 10% moisture) greater than or comparable to conventional biomass (16.3-17.6 MJ/kg for wood pellet with 7-10% moisture) but lower than fossil fuels (25-42.5 MJ/kg), and thus it is suitable to be used as a fuel in direct combustion (Kang et al., 2017; McNutt and He, 2018; Mayson and Williams, 2021). However, using pure SCG as boiler fuel may cause unstable combustion, leading to lower boiler efficiency and elevated levels of toxic gas and particle emissions (Allesina et al., 2017; Kang et al., 2017). These issues can be minimised by blending SCG with sawdust, resulting in combustion parameters similar to that of wood pellets (Limousy et al., 2012). Li et al. (2014), Kelkar et al. (2015), and Choi et al. (2017) investigated SCG valorisation via fast pyrolysis, which involves the thermochemical decomposition of biomass into bio-oil, char, and non-condensable gas at high temperatures and in an oxygen-free atmosphere. These studies demonstrated high SCG conversion, with Kelkar et al. (2015) reporting SCG conversion rates of 60%, 17.7% and 20.4% for bio-oil, char and pyrolysis gas when treated at 500˚C and 32 seconds. A recent study by Kibret et al. (2021) achieved a 95% carbon conversion at 900˚C via gasification of SCG in steam and CO_2, a process which also involves biomass decomposition under high temperatures. Besides that, studies on the anaerobic bacterial decomposition of SCG to methane rich biogas have been performed since the 1980s. This process is known as anaerobic digestion (AD). Lane (1983) and Dinsdale et al.

(1996) found SCG to have limited application as a mono-substrate of AD, failing to achieve stable biogas production due to inhibitory compounds. To circumvent this, studies such as that by Kim et al. (2016) have investigated the co-digestion of SCG with various co-substrates. As environmental and resource security issues continue to rise, there has been increasing policy focus on the adoption of a circular economy. Circular economy concept aims to promote reduction of resource consumption and waste to landfills through reusing, recycling or converting waste materials into more useful products (Department for Environment, Food and Rural Affairs (DEFRA), the Department of Agriculture, Environment and Rural Affairs (DAERA), the Welsh Government and the Scottish Government, 2020; Ng et al., 2019). The International Energy Agency (IEA) highlighted the importance of implementing a biorefinery approach (i.e. facility with integrated processes that convert biomass into value-added products) to achieve higher value generation and sustainability (Ng et al., 2017; van Ree et al., 2012). It also identified the main driver of biorefinery development as the efficient, cost-effective production of transportation biofuels. Furthermore, the IEA proposed the production of high-value products alongside biofuel products as a promising approach to reduce biofuel production costs within biorefineries (Sadhukhan et al., 2014).

SCG has been found to have great potential as a feedstock for the production of a wide range of chemicals and materials, including biofuels (Massaya et al., 2019). However, few studies have investigated the techno-economic performance of SCG biorefineries. Giller et al. (2017), Kookos (2018) and Thoppil and Zein (2021) performed economic evaluations on small-scale biodiesel production plants without the incorporation of high-value products. Kookos (2018) highlighted the importance of large plant scales to achieve competitively priced biodiesel from SCG. The study also mentioned that large scale would involve economical and practical difficulties, such as increased logistical challenges and costs for SCG collection. Thoppil and Zein (2021) emphasised that sensitivity analyses using different product price scenarios are needed to rigorously assess the viability of producing biodiesel from SCG. There is thus a lack of literature evaluating the economic and environmental performance of SCG biorefineries. These assessments are vital for

120 informing the commercial viability of SCG biorefineries and thus their future prospects (Karmee,
121 2018).

122 This study addresses the gap in literature by investigating how the economic and environmental
123 performance of SCG biorefineries are affected by the following key factors: (a) plant size; (b)
124 valorisation routes; (c) plant location relative to SCG source. Factors (a) and (b) have been selected
125 due to their significant influence on plant economics (Kookos, 2018; van Ree et al., 2012), whilst
126 (c) has been chosen to assess biorefinery economics when SCG collection costs of a large
127 biorefinery is removed by locating the plant within an instant coffee factory site. Four biorefinery
128 scenarios of different scale, valorisation routes, and locations have been analysed. The process
129 configurations focus on biodiesel production as transportation biofuels are the main drivers of
130 biorefinery development and there is a substantial amount of literature material available regarding
131 SCG valorisation to biodiesel.

132 The performances of these biorefinery systems have been compared against that of conventional
133 SCG management practices and biodiesel production processes. Additionally, the GHG emissions
134 and costs of the biorefineries have been analysed to help identify what future research efforts should
135 focus on to improve the economic and environmental performance of SCG biorefineries. The
136 novelty of this research lies in the creation of innovative conceptual biorefinery designs for SCG
137 valorisation that incorporate resource efficiency enhancement features such as multiple product
138 generation and energy integration, followed by detailed techno-economic and environmental impact
139 evaluation on different scenarios that consider plant size, valorisation routes and plant location. As
140 environmental pressure from food waste and urgency to decarbonise transport fuels escalates, this
141 research is timely and crucial to identify the most economically and environmentally compelling
142 strategies to both tackle SCG and provide society with low-carbon advanced biofuel.

2 Methodology

Literature review was performed to gain a holistic view of the SCG valorisation routes explored in previous studies. The market values of the products from these routes, chemical composition of SCG and its availability in the UK were gathered. Two biorefinery configurations were proposed. As the transportation sector is a crucial driver of biorefinery development, both configurations aimed to produce biodiesel. Configuration I was based on a well-researched SCG valorisation pathway (i.e., transesterification) combined with current practices (i.e., incineration with energy recovery). Configuration II also aimed to maximise value extracted by incorporating more novel valorisation methods for the production of high-value chemicals. Four biorefinery scenarios were generated, with different combinations of biorefinery size, design configuration, and location relative to the SCG feedstock source. For each scenario, process simulation modelling and heat integration were performed. Technical, economic, and environmental performances were then evaluated using energy and mass flow data from the simulations. The key indicators used to compare the scenarios include biodiesel yield, economic potential, net present value, cost of production per litre of biodiesel and greenhouse gas emissions.

Process Simulation Modelling: Aspen Plus V11 software was used to simulate the mass and energy flows of each system. Overall process flow diagrams were developed, with operating conditions and reaction pathways established based on experimental results from literature. The non-random two-liquid (NRTL) thermodynamic property method was used as non-ideal solutions were simulated (Gómez-Ríos et al., 2019). Distillation columns were simulated via Aspen RadFrac models with partial-vapour condensers. Pinch analysis was used to analyse the process heat recovery potential and establish targets for minimum utility consumption. The mass flowrate, enthalpy change, initial and final temperatures of hot and cold streams were extracted from the Aspen Plus simulation results and input into Aspen Energy Analyser V11 software, along with a specified global minimum temperature difference (ΔT_{min}). Using this data, a heat exchanger network (HEN) design was generated and its heat exchangers used in capital and operating cost evaluations.

Economic assessment: The economic analysis involved the evaluation of capital expenditure, operating expenditure (OPEX), and profitability. An exchange rate of 1GBP = 0.72 USD was applied. The total installed capital cost (*TCC*) of a plant was categorised into direct and indirect costs. The direct costs included the free-on-board (f.o.b.) purchase and installation costs of the biorefinery equipment. Indirect capital costs included costs for site engineering, designing, and building. To estimate *TCC*, the Lang's method was used. Equipment f.o.b cost was calculated and updated to the reference year using the CEPCI index. This is shown in Equations (1)−(2), where $COST_b$ and $COST_f$ are the equipment base and purchase costs; $SIZE_b$ and $SIZE_c$ are the size capacities of the base and current systems; R is the scaling exponent; C_r is the cost; IV_r and IV_b the index values of the reference year (2019) and base year (Davis et al., 2013). Finally, *TCC* was calculated using Equation (3), where N_{equip} is the total number of equipment and 5.03 is the Lang factor of a solid-fluid processing biorefinery (Sadhukhan et al., 2014). This method of estimating capital investment gives a 30% accuracy. However, it must be noted that the investment required for a new plant on an undeveloped site will be larger than on an existing, developed site. The annualised capital cost (*CC*) was obtained by spreading *TCC* over the plant's lifetime (*PL*) of 20 years at a discount rate (*dr*) of 10%, which is similar to the discount rates used in previous biorefinery economic analyses (Zetterholm et al., 2020). CC was estimated by using a capital recovery factor (*CRF*) as in Equations (4)−(5) (Ng and Martinez-Hernandez, 2020).

$$\frac{COST_f}{COST_b} = \left(\frac{SIZE_c}{SIZE_b}\right)^R \tag{1}$$

$$C_r = COST_f\left(\frac{IV_r}{IV_b}\right) \tag{2}$$

$$TCC = 5.03 \times \sum_{i=1}^{n=N_{equip}} C_{r,i} \tag{3}$$

$$CRF = \frac{dr(1+dr)^{PL}}{(1+dr)^{PL}-1} \tag{4}$$

$$CC = TCC \times CRF \tag{5}$$

OPEX included fixed and variable operating costs. Fixed operating cost comprised of the costs of labour, supervision, laboratory, plant overhead, maintenance, local taxes and insurance (see Appendix B, Table B.1). The number of personnel needed per shift was calculated by multiplying the number of plant processing steps with the number of personnel required per step. The annual cost of labour was calculated using Equation (6). The annual variable operating cost of the plant (*VAR*) [£/y] was calculated using Equation (7), where C_{RM} [£/y] represents raw material cost, C_U [£/y] the utilities cost, C_{WT} [£/y] the waste treatment costs and C_{CARB} [£/y] the carbon costs based on the plant's net flowrate of CO_2.. Economic viability was measured using key performance indicators such the economic potential (*EP*) [£], net present value (*NPV*) [£] and payback period. *EP* and *NPV* were calculated using Equations (8)−(9), where *h* [h] is the number of operating hours annually; r_i [kg/h] and p_i [£/kg] are the production rate and base unit price of product *i* respectively; *Np* is the total number of products; *OC* [£/y] is the annual operating costs and C_f [£] refers to the cash flow in a particular year (Ng et al., 2013).

$$\text{Cost of personnel (£/year)} = \text{Number of personnel per shift} \times 5 \text{ shifts} \times 40 \text{ hours/week} \times 52 \text{ weeks/year} \times \text{Hourly wage} \quad (6)$$

$$VAR = C_{RM} + C_U + C_{WT} + C_{CARB} \quad (7)$$

$$EP = h \sum_{i=1}^{i=Np} r_i p_i - CC - OC \quad (8)$$

$$NPV = \sum_{n=0}^{n=PL} \frac{C_f}{(1+dr)^n} \quad (9)$$

Environmental impact assessment: The system boundary was defined (see Figure 1) and inventory analysis was performed.

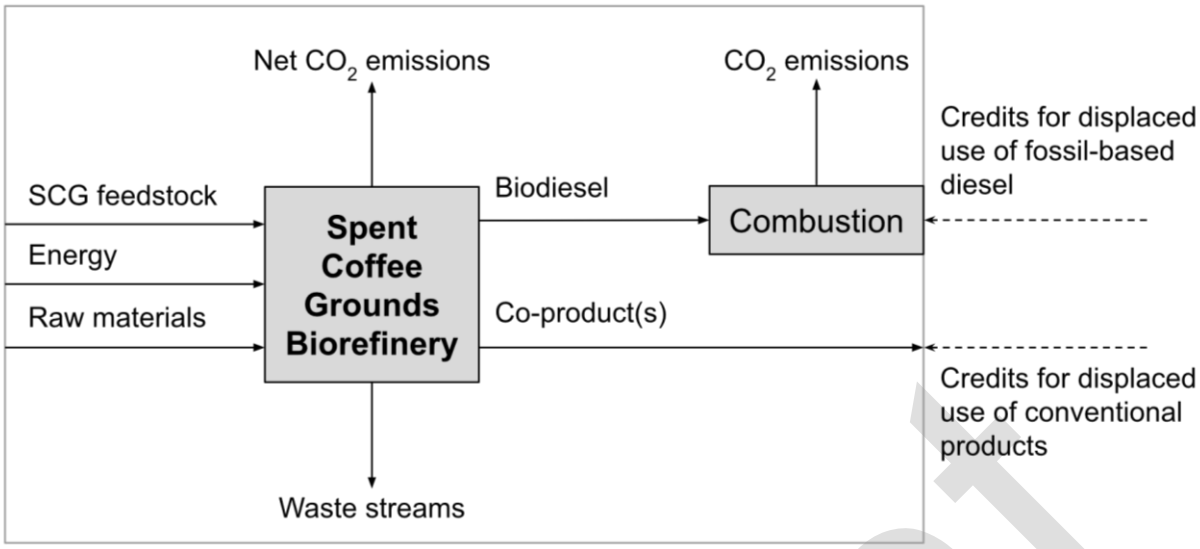

Figure 1. System boundary for the SCG biorefinery.

Input and output stream data were compiled from simulation results. CCaLC2 (a life cycle assessment software developed by the University of Manchester) was used to estimate the GHG emissions of these input and output flows. Using ISO 14067 standards (International Organization for Standardization, 2018), the net GHG emissions of the SCG biorefinery was calculated using Equation (10), where E_{RM}, E_P, E_{COMB}, E_{ENERGY}, E_{TRAN}, E_{WT} are the emissions from the raw materials used, the plant processes, the combustion of the biodiesel produced, the energy consumed, SCG transport, and waste treatment. Emission credits (GHG removals) for the electricity exported to the grid (CR_E) and displacement of conventional production of the products generated from SCG (CR_P) are applied.

$$\text{Net GHG} = E_{RM} + E_P + E_{COMB} + E_{ENERGY} + E_{TRAN} + E_{WT} - CR_E - CR_P \quad (10)$$

Sensitivity analysis: Price sensitivity analysis was performed on all scenarios using methodology outlined by Ng et al. (2013). A percentage change in price (Δ%) was defined and three sets of prices were generated for each product: the base price (subscript 0), a price Δ% lower than the base price (subscript –Δ%), and a price Δ% higher than the base price (subscript +Δ%). For *Np* number of products, there are *n* possible combinations of prices. MATLAB was used to calculate the revenues of each of these combinations using the equation shown in Equation (11), where the price scenarios matrix was multiplied by production rates (*r*) to give *n* revenue scenarios. The capital and operating

costs (assumed to be fixed) were subtracted from each element of the revenue column vector produced in Equation (11) to give the *EP* for each price scenario.

An economic risk is a change in revenue due to change in the combination of product prices. Classes of economic risks were defined in terms of the percentage change in *EP* relative to the *EP* calculated from base prices. The probability of a class of economic risk occurring is the ratio of the number of combinations that produce that class of economic risk to the total number of combinations.

$$\begin{bmatrix} p_{1,0} & p_{2,0} & \cdots & p_{\mathrm{Np},0} \\ p_{1,+\Delta\%} & p_{2,+\Delta\%} & \cdots & p_{\mathrm{Np},+\Delta\%} \\ p_{1,-\Delta\%} & p_{2,-\Delta\%} & \cdots & p_{\mathrm{Np},-\Delta\%} \\ \vdots & \vdots & \vdots & \vdots \end{bmatrix}_{n\times Np} \begin{bmatrix} r_1 \\ r_2 \\ \vdots \\ r_{Np} \end{bmatrix}_{Np\times 1} = \begin{bmatrix} p_{1,0}\,r_1 + \ldots + p_{Np,0}\,r_{Np} \\ p_{1,+\Delta\%}r_1 + \ldots + p_{Np,+\Delta\%}r_{Np} \\ p_{1,-\Delta\%}r_1 + \ldots + p_{Np,-\Delta\%}r_{Np} \\ \vdots \end{bmatrix}_{n\times 1} \quad (11)$$

3 SCG Biorefinery Configurations: Modelling and Integration

This section details the two biorefinery configurations proposed. Process description and mass and energy balances are presented. Detailed stream tables, process flowsheets and the specifications used in Aspen Plus process models are provided in Appendix C.

3.1 Proposed SCG Configurations

In the biorefinery configuration descriptions, a wet SCG plant input of flowrate 5767 kg/h at 20˚C was employed based on SCG produced by London coffee establishments (see Section 3.2). Configuration I produces biodiesel from extracted SCG oil, with electricity generated as a co-product due to the combustion of defatted SCG. Heat from the combustion is exported to a heat network. Configuration II produces biodiesel as well as succinic acid (SA), aromatics (vanillin, vanillic acid, guaiacol, acetovanillone), carboxylic acids (formic acid, acetic acid) and polyhydroxybutyrate (PHB) bioplastic. In contrast to Configuration I, no combustion is performed. Heat integration in both configurations uses a ΔT_{min} of 15˚C.

3.2 SCG Feedstock

SCG feedstock composition: SCG feedstock was modelled with a moisture content of 66% (Caetano et al., 2014). Dry mass compositional data and their representative Aspen Plus components are presented in Table 1 (Obruca et al., 2015). Further details about the component data used in the simulations can be found in Table A.1 of Appendix A.

Table 1. Chemical composition of SCG dry mass and the representative components adopted in Aspen Plus (Obruca et al., 2015).

SCG Component	Representative component adopted in Aspen Plus	Content [(i)] (wt%)
Cellulose	Cellulose	10.95
Hemicellulose	Cellulose	31.83
Lignin	Vanillin	27.00
Oil (triglycerides)	Triolein	11.35
Oil (free fatty acids)	Oleic acid	3.65
Protein [(iv)]	Glutamic acid [(ii)]	10.70
Polyphenol	Caffeic acid [(iii)]	2.50
Caffeine	Caffeine	0.02
Ash [(iv)]	Calcium Oxide	2.00
Moisture	Water	66

Note:

[(i)] All components are in wt% of dry mass except for water.

[(ii)] Glutamic acid found to be major component of SCG protein (Martinez-Saez et al., 2017).

[(iii)] Caffeic acid identified in SCG (Panusa et al., 2013).

[(iv)] Protein and ash treated as insoluble compounds and did not partake in any chemical reaction (Humbird et al., 2011).

SCG feedstock availability: The SCG used in the scenarios was obtained from either London coffee establishments or Nestlé's coffee factory in South Derbyshire, UK. The parameters used to calculate the amount of SCG produced in London coffee shops are summarised in Table A.3 of Appendix A. The total amount of wet SCG produced in London coffee establishments was calculated using Equation (A.1), giving a value of 46,136 t/y. On the other hand, the annual wet SCG production rate from Nestlé's coffee factory was calculated as 105882 t/y using Equation (A.2) and the parameters in Table A.4.

3.3 Biorefinery Scenarios

This section outlines four SCG biorefinery scenarios based on Configurations I and II, described in Sections 3.5 and 3.5. The biorefinery plants in Scenarios A, B and D were taken to be 70 km away from their SCG source, based on the average distance between the centre of Greater London and its perimeter. Other parameters used for SCG transport are included in Table A.2 in Appendix A. Besides this, input SCG feedstock of these 3 scenarios enters the biorefineries at 20˚C. Scenario A is considered the base case scenario. Here, Configuration I processes all the SCG generated in London coffee shops, producing biodiesel and electricity. The parameters used in Scenario B are identical to those of Scenario A except for the use of all the SCG produced from the Nestlé coffee factory. On the other hand, Scenario C assumes the biorefinery of Scenario B is located within the coffee factory site and that the SCG is delivered directly from the factory's coffee brewing process, entering the biorefinery at 80˚C. SCG transportation is excluded in Scenario C and the SCG feedstock is thus obtained at no cost. Scenario D uses parameters identical to that of Scenario A apart from the use of Configuration II.

3.4 Configuration I

The flow diagram is illustrated in Figure 2.

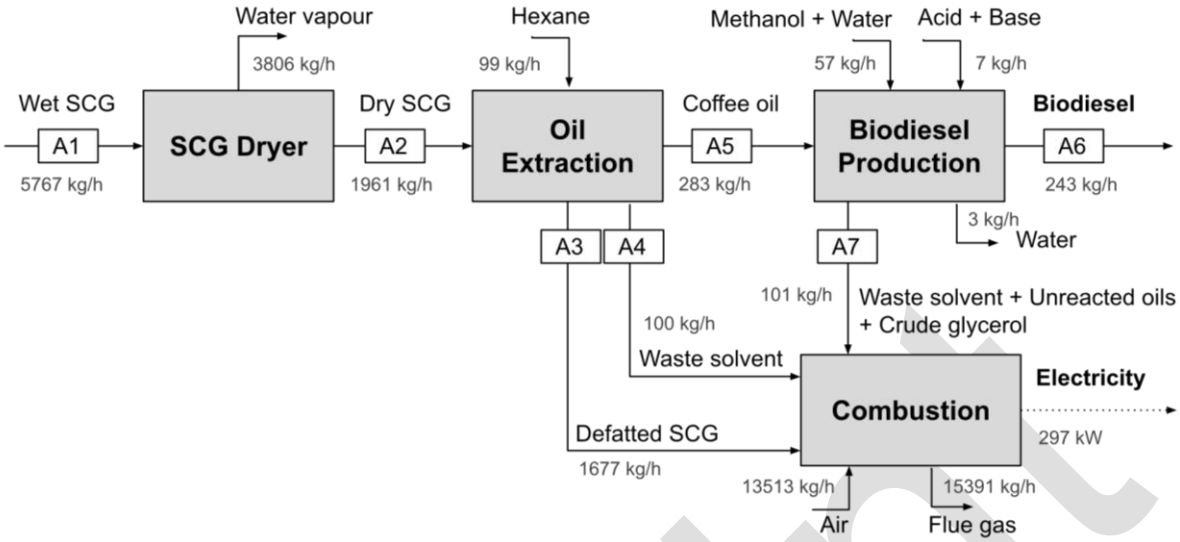

Figure 2. Flow diagram of SCG biorefinery Configuration I.

SCG drying and oil extraction: Wet SCG (stream A1) is dried at 102°C to reduce moisture content from 66% to 0%. As moisture reduces oil solubility in the hydrophobic solvent, the absence of water is crucial to achieve high oil extraction yields in the following process (Najdanovic-Visak et al., 2017). Solvent extraction of the SCG oil content (FFAs and triglycerides) is performed on dry SCG (stream A2) at 60˚C, with process parameters summarised in Table C.1 of Appendix C (Najdanovic-Visak et al., 2017). *n*-hexane is used as it has been found to give the highest yield of oil (Somnuk et al., 2017). The liquid solvent/oil mixture and the solid defatted SCG are separated via centrifugation and the solvent is removed in a flash vessel at 0.1 bar and 80°C. The separated solvent is recycled for further use in oil extraction. The defatted SCG (stream A3) and waste solvent stream from the recycle loop purge (stream A4) are combusted whilst the extracted coffee oil (stream A5) is used in biodiesel production.

Biodiesel production from SCG oil: Oil (stream A5) enters a two-step process to produce biodiesel (Efthymiopoulos et al., 2018; Hochegger et al., 2019; Saratale et al., 2020). Esterification is performed before transesterification to esterify the FFA and minimise soap formation. Table C.2 summarises the process parameters used. During the esterification process described in Equation (12), methanol (CH_3OH) reacts with FFA ($C_{18}H_{34}O_2$) to form biodiesel ($C_{19}H_{36}O_2$) with sulphuric

acid as the catalyst. The products of esterification undergo sodium hydroxide (NaOH) catalysed transesterification where biodiesel and glycerol ($C_3H_8O_3$) are formed, as shown in Equation (13).

$$C_{18}H_{34}O_2 + CH_3OH \rightleftharpoons C_{19}H_{36}O_2 + H_2O \quad (12)$$

$$C_{57}H_{104}O_6 + 3CH_3OH \rightleftharpoons 3C_{19}H_{36}O_2 + C_3H_8O_3 \quad (13)$$

The transesterification products enter a flash vessel at 162˚C and 1 bar to recover methanol for recycling. The bottom products of the flash vessel are washed in acidic water to neutralize the base catalyst used in transesterification. Next, centrifugation separates biodiesel, methanol, and hexane from the other denser liquids. Two flash vessels at 0.1 bar and 167˚C and 270˚C purify the biodiesel, producing biodiesel (stream A6) to EN14214 European standards (Tsoutsos et al., 2019). The crude glycerol produced from transesterification, methanol recycle-loop purge and other waste organic streams consisting of unreacted oils (stream A7) are combusted.

Combustion of defatted SCG and waste streams: The combustion of streams A3, A4 and A7 was modelled using a stoichiometric reactor at 500˚C and 1 bar. Flue gas exiting the combustion chamber at 500˚C is used to pre-heat boiler feed water from 20˚C to 102˚C, reducing the gas temperature to 112˚C. The heat from combustion reactor is used to generate steam of 480˚C and 135 bar from the pre-heated water. The steam drives a turbine of 90% isentropic efficiency and a pressure drop of 107.5 bar, generating a total of 1085 kW of electricity. Of this, 788 kW is used by plant processes and the remaining 297 kW is exported to the grid. Heat from the steam leaving the turbine (247˚C and 27.5 bar) and the flue gas (112˚C) is extracted and exported to a heating network. The flue gas contains 3528 kg/h of CO_2, of which 86% is due to the combustion of SCG material.

Validation of simulation results: In this configuration, 5767 kg/h of SCG at 66% moisture produces 283 kg/h of oil and 243 kg/h of biodiesel product. This corresponds to a yield of 0.86 kg biodiesel per kg coffee oil, which is in close agreement with the average of yields found from literature, i.e. 0.84 kg biodiesel/kg oil (Abdelaziz et al., 2020, 2019).

3.5 Configuration II

The process block diagram was illustrated in Figure 3.

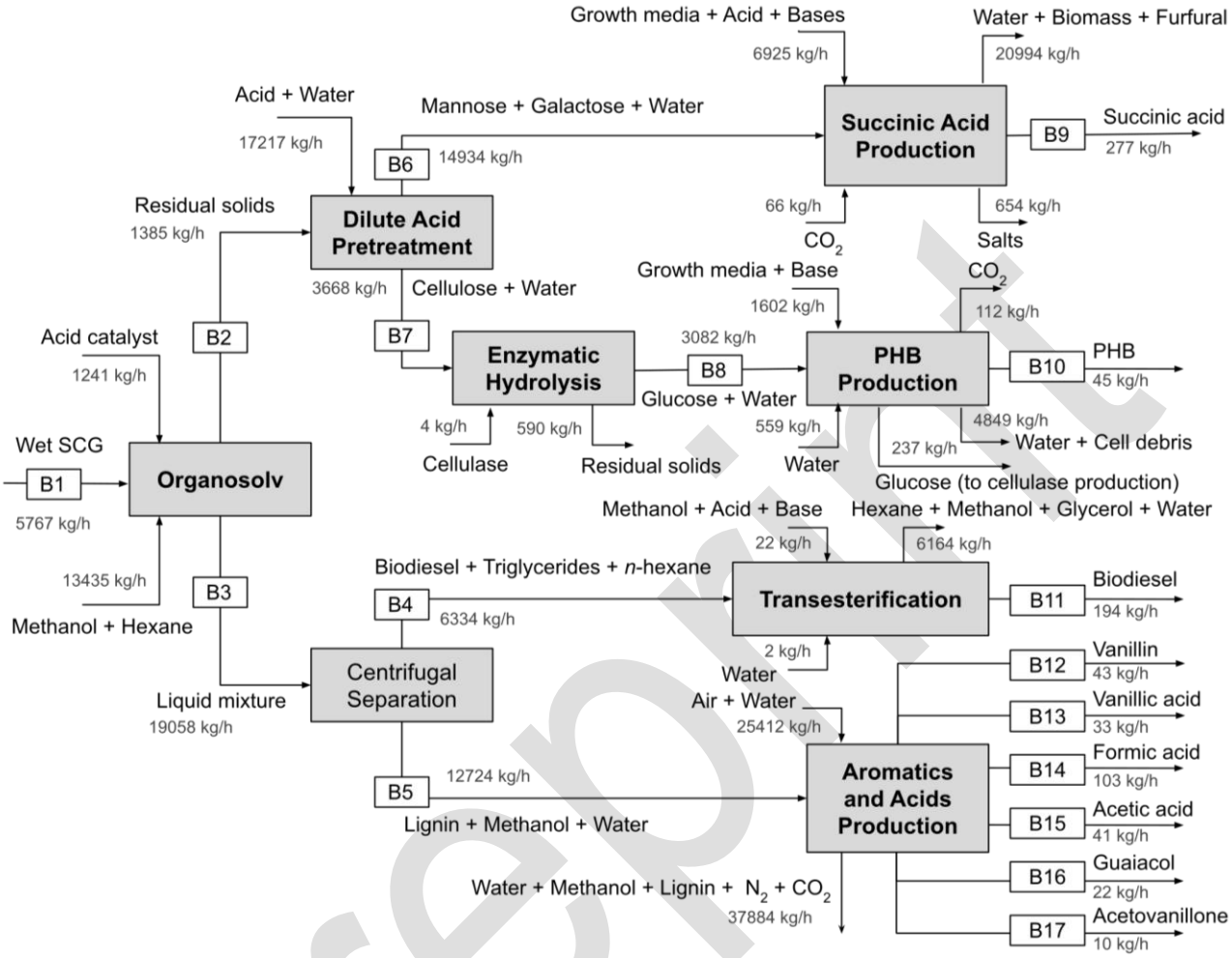

Figure 3. Flow diagram of SCG biorefinery Configuration II.

Pre-treatment: To isolate lignin, Organosolv pre-treatment was selected as it is the only experimentally validated technique of SCG lignin isolation found in literature (Lee et al., 2019). The process conditions used are adopted from said study. The wet SCG feedstock (stream B1) does not undergo pre-drying as the high moisture content promotes solvent penetration into SCG during pre-treatment, therefore increasing delignification rates (Hochegger et al., 2019).

Solvents *n*-hexane and methanol are added to a reactor at 161˚C and 1 bar, along with sulphuric acid as the catalyst. Under these conditions, lignin dissolves in methanol, while triglyceride and FFA are simultaneously extracted into *n*-hexane. The sulphuric acid catalyses the esterification of the extracted FFA, forming biodiesel. The solid residues consisting of mainly hemicellulose and

cellulose fibres are removed using a filter, forming stream B2. The remaining liquid mixture (stream B3) is separated into stream B4 (containing solubilised lignin) and stream B5 (containing mainly biodiesel and triglycerides) via centrifugation. Lignin and biodiesel recoveries of 56% and 62.4% are obtained from the Organosolv reactor (Lee et al., 2019). Oil extraction yield was taken as 78 wt% (Efthymiopoulos et al., 2018).

Dilute acid pre-treatment and enzymatic hydrolysis: The solid residues of stream B2 are slurried in dilute sulphuric acid and treated at 163˚C and 1 bar (Mussatto et al., 2011). Under these conditions, hemicellulose is converted to its monomeric sugars. After pre-treatment, the solid cellulose and hemicellulose hydrolysate are separated via centrifugation, after which the solids are washed with water to remove any residual soluble sugars and fermentation inhibitors (sugar degradation products). The water stream from this washing stage is merged with the hemicellulose hydrolysate and the resulting stream is detoxified using a granular activated carbon column to remove HMF and furfural formed (Nieder-Heitmann et al., 2019). The column output stream is sent to a neutralisation reactor (38˚C, 1 bar) where calcium hydroxide neutralises the remaining acid. The resulting salt is precipitated and filtered out, leaving a hemicellulose sugar-rich stream (stream B6) utilised in SA production. On the other hand, the solid cellulose residues (stream B7) from the dilute acid pre-treatment are subjected to enzymatic hydrolysis at 48°C. Here, cellulase enzymes convert the cellulose fibres into glucose monomers and small traces of soluble gluco-oligomers. Solid residues of unreacted lignin, proteins, cellulose, and other compounds are removed from the aqueous glucose stream (stream B8) via centrifugation.

SA production from hemicellulose: The detoxified, neutralised aqueous solution of hemicellulose sugars (stream B6) is utilised in SA production using the bacteria *Actinobacillus succinogenes* (Nieder-Heitmann et al., 2019). Like PHB production, growth and synthesis reactors are used. Both reactors operate at 38˚C. With 10% of stream B6 directed to the growth reactor, the remaining is sent to the synthesis block, after passing through flash drums to concentrate the hydrolysate stream to 200 g/L of sugars (Nieder-Heitmann et al., 2019).

The products of the synthesis reactor are filtered to remove cells and the liquid product stream sent to an adsorption tower. An adsorption tower using resin NERCB 09 is used due to its high SA selectivity and average recovery of 96% (Li et al., 2009). After adsorption, the adsorbent is easily regenerated using NaOH solution. As SA reacts with the base to form sodium succinate, sulphuric acid is added to the reactor, forming sodium sulphate and SA. A patented process involving selective precipitation of sodium sulphate is applied to recover the SA (Fujita and Wada, 2008). Finally, a distillation column removes water, producing the SA product stream B9.

PHB production from cellulose: A fraction of the glucose-rich stream B8 is diverted as feed for the cellulase production plant at a rate of 3.9 kg/h of glucose per kg/h of cellulase required (Humbird et al., 2011). The remaining glucose is used for PHB production. Although there exists a variety of microbes with the ability to produce PHB intracellularly, the use of recombinant *E. coli* was chosen as it produces PHB during both growth and synthesis phases, resulting in lower residence times and capital costs (Nieder-Heitmann et al., 2019). The PHB production process consists of growth and synthesis phases, product separation and purification. The glucose stream from the enzymatic hydrolysis of cellulose is split into two streams, with 9.5% sent to the growth reactor and the remaining to the synthesis reactor. Before these glucose streams enter the reactors, they are either mixed with water or undergo evaporation to achieve glucose concentrations of 20 g/L and 700 g/L for the growth and synthesis reactors, respectively. The growth reactor produces a population of microorganisms from a stock dormant culture, sugar, and ammonia for use in PHB production in the synthesis reactor. The microbial cells are sent to the synthesis reactor, where concentrated glucose (700 g/L) is fed for continued bacterial growth and intracellular PHB production. A centrifuge separates the cells containing PHB from the fermentation broth. After a water wash at 30˚C, the cells are lysed in a blending tank at 30˚C containing a 0.2 M NaOH solution to release the PHB within the cells. The PHB crystallises upon exposure to the solution (Nieder-Heitmann et al., 2019). Finally, the crystalline PHB is subjected to a final water wash and

centrifugation to remove any residual cell material before being atomized into particles using a spray dryer, forming stream B10.

Biodiesel production from oil: Stream B4 is subjected to identical transesterification and biodiesel purification processes as in Configuration I. However, *n*-hexane is first separated from the lipids using a flash drum at 75˚C and 0.06 bar. Biodiesel (stream B11) is produced.

Production of aromatic compounds and acids from lignin: The soluble lignin of stream B5 is precipitated out via the addition of water and the solid lignin formed is separated using a filter. This lignin and compressed air enter an oxidative depolymerisation reactor (160˚C, 8 bar) (Fujita and Wada, 2008; Li et al., 2009) where lignin reacts with oxygen to produce vanillin, vanillic acid, formic acid, acetic acid, guaiacol, and acetovanillone (streams B12-B17), along with CO_2. Unreacted lignin is removed via filtration and recycled back to the depolymerisation reactor to maximise production of the high-value chemicals. The products in the liquid stream are isolated using a novel hydrophobic membrane separator that has been shown to achieve perfect separation of organic and aromatic compounds from aqueous mixture (IEA Bioenergy, 2021; Phillips et al., 2019). The membrane unit thus was modelled using a separator block with perfect separation of organic compounds. The products in the organic phase output stream of the membrane separator are separated using a series of distillation columns under vacuum conditions to give product streams B12-B17 of 98-99% purity.

4 Results and Discussion

The parameters and assumptions used in the scenarios were outlined in Section 4.1. Performance analyses explored the influence of size, location and products on the economic and environmental performance of a biorefinery, presented in Section 4.2. The biorefinery GHG emissions were compared against that of conventional SCG management practices. Biorefinery performances were

also compared against that of conventional biodiesel. Section 4.3 provides insights on the future prospects of SCG biorefineries and recommendations for future studies.

4.1 Parameters and Assumptions for Scenarios

Parameters for performance evaluation: To determine economic performance, *h* was taken as 8000 hours. For labour cost calculations (Equation (6)), Configuration I involved 3 processing steps and was considered automated, requiring one personnel per step. Configuration II had 6 processing steps, with 3 personnel required per step due to the complexity of the plant design. The *EP* and *NPV* were calculated using Equations (8)−(9), where the values of *Np* were 3 and 9 for Configuration I and II respectively. Price sensitivity analysis was performed (see Section 2) with price fluctuations (Δ%) of 10%. The unit product prices are summarised in Table D.1 of Appendix D. The cost of production of biodiesel (£/L) was calculated using Equation (14).

$$\text{Biodiesel cost} = \frac{\text{Total annual production cost}}{\text{Litres of biodiesel produced annually}} \times \frac{\text{Biodiesel revenue}}{\text{Total revenue}} \quad (14)$$

Net GHG values were calculated using Equation (10) and net heat and electricity consumptions were calculated by subtracting heat and electricity consumed from that produced by SCG combustion.

4.2 Performance Analysis

The parameters and key performance indicators of each scenario are summarised in Table 2, where negative values of net heat or electricity consumption represents net generation and subsequent export to heat networks or the electrical grid.

Table 2. Parameters and key performance indicators of the scenarios analysed.

	Scenario A	**Scenario B**	**Scenario C**	**Scenario D**
Brief Description	Config I London SCG Off-site	Config I Factory SCG Off-site	Config I Factory SCG On-site	Config II London SCG Off-site
Parameters				
Configuration	I	I	I	II

SCG feedstock source	London shops	Nestlé factory	Nestlé factory	London shops
SCG transport distance (km)	70	70	-	70
SCG feedstock temperature (˚C)	20	20	80	20
SCG feedstock flowrate (t/y)	46136	105882	105882	46136
Technical Performance Indicators				
Biodiesel yield (kg biodiesel/t SCG processed)	42.10	42.10	42.10	33.60
Net heat consumption (MJ/t SCG processed)	− 3392.93	−3501.58	−3522.28	7575.38
Net electricity consumption (MJ/t SCG processed)	−185.12	−195.01	−195.01	144.84
Economic Performance Indicators				
Economic potential, *EP* (million £/y)	−0.46	0.12	0.62	2.97
Net present value, *NPV* (million £)	−3.90	−0.42	3.07	15.19
Payback period (y)	16.6	8.0	6.3	6.2
Cost of biodiesel production (£/L)	1.02	0.81	0.72	0.69
Environmental Performance Indicators				
GHG emissions (kg CO_2-eq./t SCG processed)	81.21	80.98	78.61	2233.00

Figure 4 presents the economic and environmental performance of the scenarios. The cumulative cash flows of the scenarios are illustrated in Figure 4 (a), where *TCC* is evenly divided between years −2 to 0. Positive and negative *NPV* values indicate profitable and loss-making projects, respectively. The payback periods of Table 2 are the number of years required to recover the *TCC* investment. These are represented by the x-axis intercepts on Figure 4 (a) and are a measure of the plant's attractiveness as an investment. Revenues are categorised by product sales in Figure 4 (b) and cost breakdowns of the scenarios are shown in Figures D.1−D.3. The results of the price sensitivity analysis are illustrated in Figure 4 (c), with the legend indicating the classes of economic risk. For example, '0 to −20%' economic risks referred to price combinations that resulted in a 0 to 20% decrease in *EP* relative to the *EP* generated from base prices. For Scenario A, none of the price combinations resulted in a positive value for *EP*, while all the price combinations of Scenarios C and D generated positive *EP*.

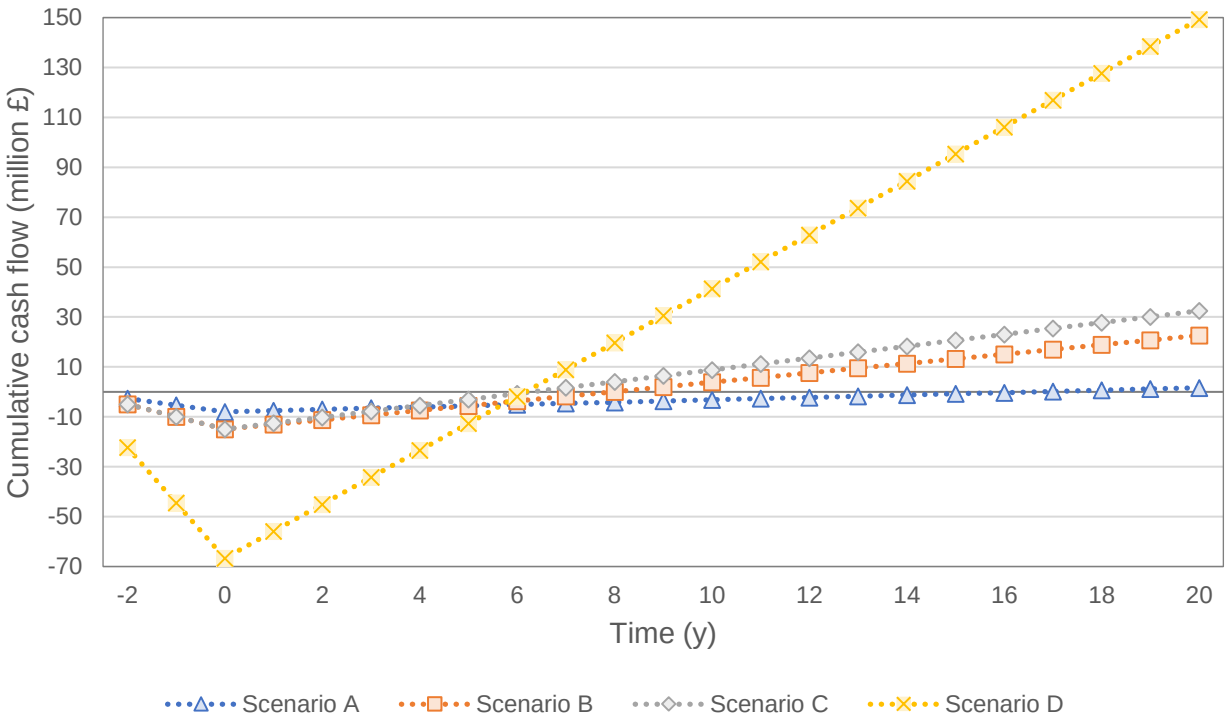

442

443 (a)

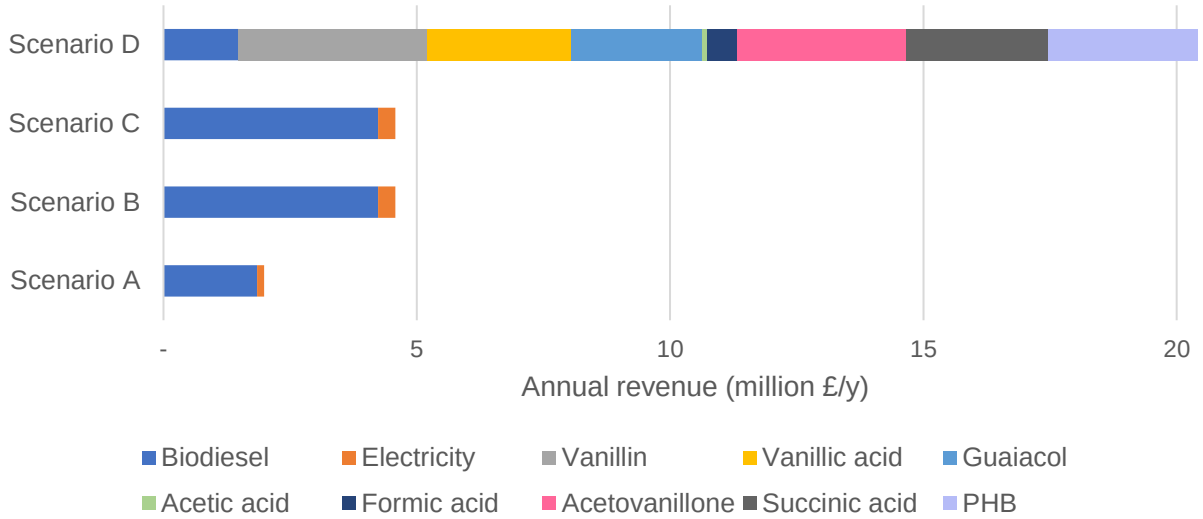

444

445 (b)

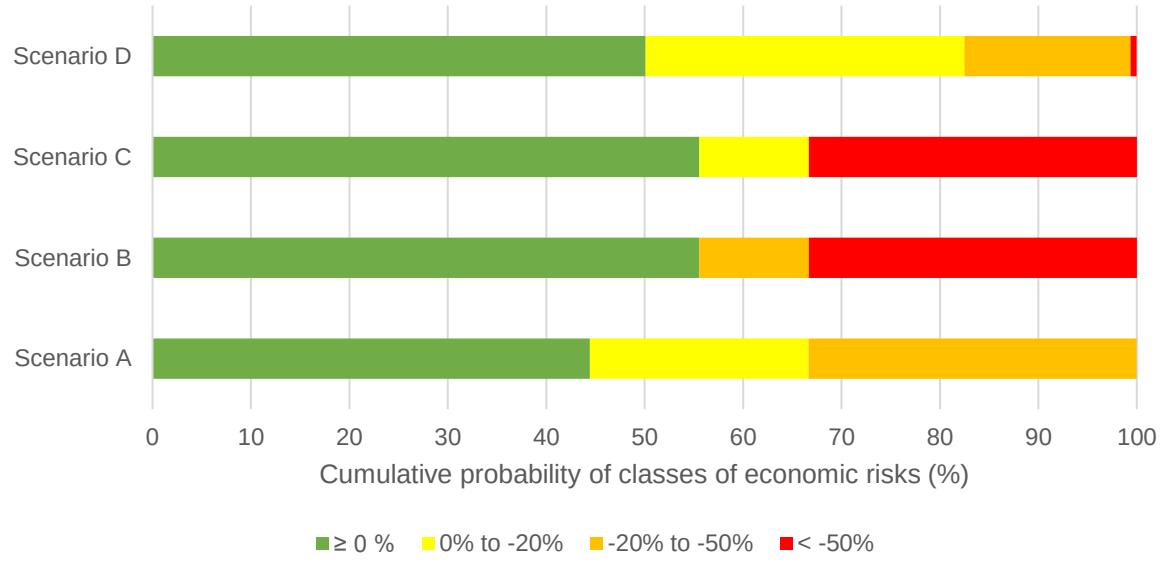

446

447 (c)

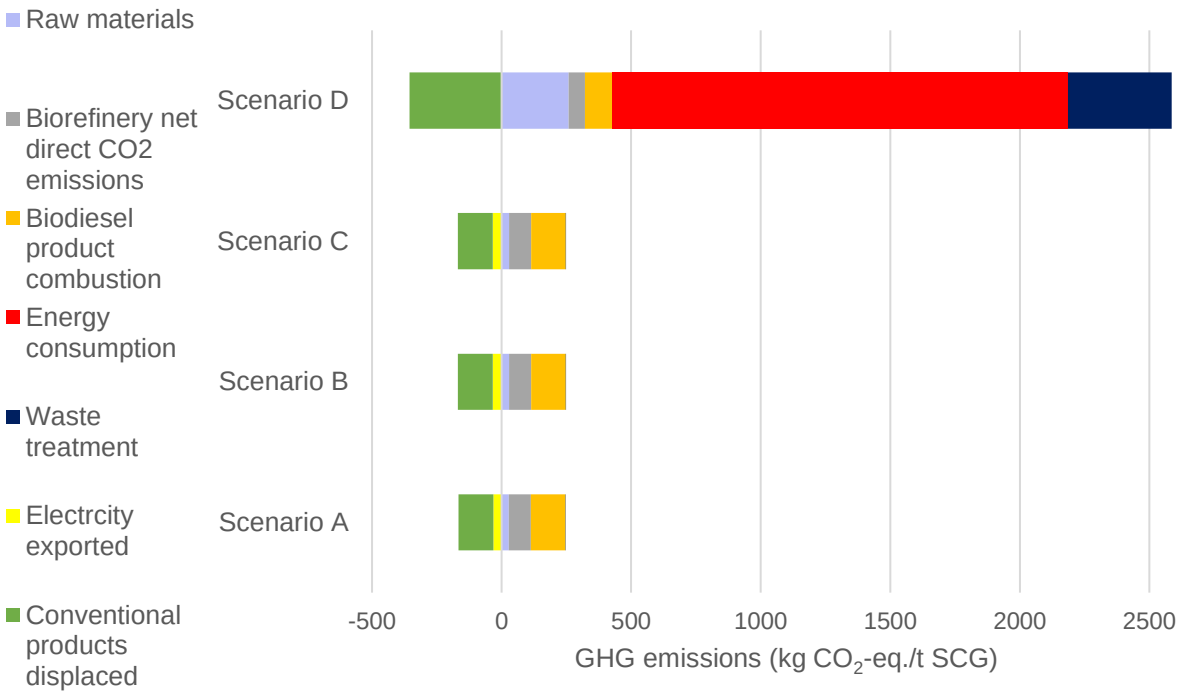

448

449 (d)

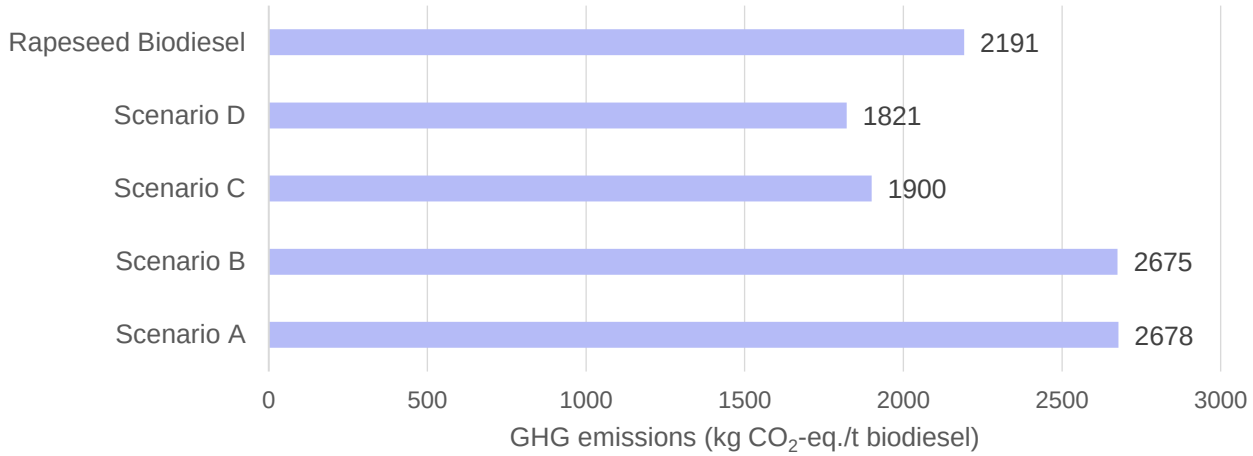

(e)

Figure 4. Economic and environmental performance of scenarios analysed. (a) Cumulative cash flows for the plant's 20 years of operation; (b) Classification of revenues by product sales; (c) Likelihood of different classes of economic risk; (d) Classification of GHG emissions per tonne of SCG processed; and (e) GHG emissions per tonne of biodiesel produced.

Plant size: The impact of increasing biorefinery size was investigated by comparing the performances of Scenario A and B, with SCG feedstock flowrates of 46136 and 105882 t/y, respectively. Scenario A generates a negative *NPV* value of −£3.9 million, implying that this scenario is not economically compelling. Increasing the plant size by 2.3 times to that of Scenario B still resulted in an economically unviable plant, with a *NPV* of −£0.42 million (Table 2). However, the increase in *NPV* along with the reduction in payback period from 16.6 to 8.0 years (Figure 4 (a)) indicates that Scenario B is a more attractive investment than Scenario A. The cost of biodiesel production was reduced by 18% from 0.88 to 0.72 £/L (Table 2). This improved economic performance aligns with previous hypotheses that larger scale of SCG biorefineries is required to result in an economically viable production (Giller et al., 2017). Besides that, a price sensitivity analysis of both scenarios (Figure 4 (c)) reveals that Scenario B has a 11% greater likelihood of ≥0% economic risks when product prices fluctuate from their base levels. A ≥0% ecnomic risk refers to an increase or no change in *EP* relative to the *EP* generated at base prices, thus requiring no modification to the biorefinery processes. The likelihood of $< -50\%$ economic risks rose from

0% (Scenario A) to 33% (Scenario B). This type of economic risk would greatly reduce *NPV* and thus would require plant process modifications to minimise its large negative economic impact. Generally, the greater the likelihood of $< -50\%$ economic risks, the higher the economic risk of the scenario. Thus, increasing the biorefinery size results in an overall rise in the plant's economic risk.

On the other hand, environmental performance (see Figure 4 (d)) does not improve by increasing biorefinery size, with the GHG emissions of Scenario B a mere 0.3% lower than that of Scenario A. Biodiesel yield per tonne of SCG processed is not affected while the net heat and electricity generated per tonne of SCG increase with biorefinery size.

Biorefinery location: Scenarios B and C were compared to examine the impact of biorefinery location relative to the SCG source. Locating the biorefinery within Nestlé's Derbyshire coffee factory site results in significant improvement in economic performance, with *NPV* growing by 9.3 times to £3.1 million, a 1.7-year reduction in payback period and a 11.1% reduction in biodiesel production cost. These findings demonstrate the significance of a centralised processing facility on the economic performance of SCG valorisation, as concluded by Kookos (2018)**.** Economic risk also decreases, with around a tenth of price combinations generating economic risks of 0% to -20% instead of -20% to -50%. However, there remains a 33% likelihood that 10% product price fluctuation results in $< -50\%$ economic risk, indicating that the economic viability of Scenario C is still vulnerable to market price fluctuations. Besides that, the omission of SCG transport results in a 30% reduction in raw material cost and a 3% reduction in GHG emissions. While biodiesel yield and net electricity consumption remain unchanged, net heat generated increases slightly by 0.5% as the SCG feedstock enter at 80˚C, resulting in lower SCG drying heat requirements.

Biorefinery products: The impact of producing high-value chemicals was assessed by comparing Scenarios A and D. Scenario D has excellent economic performance, with a *NPV* of £15.2 million and a payback period of 6.2 years. The cost of biodiesel production decreases by 4% from 0.72 £/L to 0.69 £/L due to biodiesel comprising a much smaller proportion of total revenue and use of

Equation (14). This result supports the IEA's proposition that producing high-value products alongside biofuels would lower biofuel production costs (van Ree et al., 2012). As illustrated in Figure 4 (b), almost 90% of the annual revenue generated by Scenario D is evenly distributed between sales from vanillin, vanillic acid, guaiacol, acetovanillone, SA and PHB. This even distribution of revenue across many products leads to the reduced economic risk seen in the results of the sensitivity analysis in Figure 4 (c). In contrast, Scenario A has much higher economic risk due to biodiesel sales constituting 93% of its revenue. Thoppil and Zein (2021) also found the *NPV* of SCG biorefinery to be highly sensitive to product prices when products are of limited range and low value.

However, the economic performance of Scenario D is at the cost of greater environmental impact, with GHG emissions increasing by 27.5 times to 2233 kg CO_2-eq./t SCG (Figure 4 (d)). Steam generation and electricity usage constitute 52% and 18% of the total emissions from the plant, respectively. These emissions have been grouped and labelled as 'energy consumption' in Figure 4 (d). For its GHG emissions/t SCG to match that of Scenario A, the energy consumption of Scenario D would have to be reduced by at least 22%. As Scenario D does not involve on-site energy recovery via combustion, it results in net electricity and heat consumption 3.2 and 1.8 times that of Scenario A. Besides that, Scenario D results in a biodiesel yield around 20% less than Scenario A due to the lower biodiesel yields of the Organosolv pre-treatment.

Conventional SCG management practices: The environmental impacts of Scenarios A and D were compared against that of the two most widespread SCG management practices in the UK: EfW and landfilling. Schmidt et al. (2020) found the GHG emissions of SCG EfW and landfill facilities with energy recovery to be −435 kg CO_2-eq./t SCG and 525 kg CO_2-eq./t SCG, respectively. Neither Scenario A nor D have GHG emissions as low as EfW practices. Scenario A produces around 85% less GHG emissions than landfilling while Scenario D produces more than 4 times the GHG emissions of landfilling. Note that Scenarios B and C were excluded from this comparison due to the similarity of their GHG emissions with that of Scenario A.

Conventional biodiesel production: The GHG emissions of Scenarios A to D were compared against that of conventional biodiesel production in Europe. Rapeseed oil is the dominant feedstock for EU biodiesel production, constituting 39% of total production in 2018 (Phillips et al., 2019). The GHG emissions generated from rapeseed biodiesel produced via esterification was reported by Pehnelt and Vietze (2012), whose study excluded emissions from the transportation of the biodiesel product to the consumer, biodiesel combustion and waste treatment. A functional unit of 1 tonne of biodiesel production was used. Adopting identical system boundaries and functional unit, the GHG emissions generated by biodiesel production was calculated by summing the emissions from SCG collection, Organosolv pre-treatment and transesterification. For the collection and pre-treatment, the GHG emissions generated from biodiesel production were calculated using Equation (15), where 'Process GHG' refers to the total GHG emissions of each process.

$$\text{GHG from biodiesel production} = \text{Process GHG} \times \frac{\text{Biodiesel revenue}}{\text{Total revenue}} \quad (15)$$

The GHG emissions of the scenarios were compared against that of rapeseed biodiesel as shown in Figure 4 (e). The GHG emissions in Scenario C (1900 kg CO_2-eq./t biodiesel) are 29% lower than that of Scenario B (2678 kg CO_2-eq./t biodiesel) as it excludes transportation of the 23.8 tonnes of SCG required to produce 1 tonne of biodiesel. Besides that, Scenarios C and D produce GHG emissions that are 13% and 17% lower than rapeseed biodiesel.

The relatively low emissions of Scenario D are due to the exclusion of waste treatment emissions (which constitute 18% of total GHG emissions/t SCG) and use of Equation (15) (as biodiesel revenue represents just 7% of total revenue). Although the GHG emissions/t biodiesel appear promisingly low, Figure 4 (d) shows that total GHG emissions generated by Scenario D are 7 times greater than the emissions credited from displacing the use of conventional products. Thus, producing these high-value chemicals (e.g., vanillin, PHB) via the SCG biorefinery results in greater GHG emissions than conventional production methods.

According to the IEA, the production cost of conventional biodiesel ranges from 0.66−0.86 £/L (International Energy Agency, 2012). All the scenarios apart from Scenario A result in biodiesel production costs that are within this range. The results from this comparison indicate that SCG biorefineries could potentially be used to meet growing biodiesel demands.

4.3 Insights and Recommendations

From the economic and environmental evaluations performed in Section 4.2, Scenario C was found to be the most promising SCG biorefinery strategy. Although its *NPV* of £3.1 million is around 5 times lower than that of Scenario D, its GHG emissions (79 kg CO_2-eq./t SCG processed or 1900 kg CO_2-eq./t biodiesel) are 28 times lower than Scenario D, 7 times lower than SCG landfilling (525 kg CO_2-eq./t SCG) and 13% lower than that of conventional rapeseed biodiesel (2191 kg CO_2-eq./t biodiesel). It also has a biodiesel cost of production of 0.72 £/L, which is within the range estimated by IEA (0.66−0.86 £/L). Furthermore, a practical advantage of using SCG from a coffee factory is a more consistent feedstock flowrate and composition than SCG from coffee establishments, resulting in fewer changes in operating conditions and product output. However, the economic viability of Scenario C is sensitive to product price fluctuations, with 55.6% and 33.3% likelihoods of $\geq$0% and $<-50\%$ economic risks, respectively (Figure 4 (c)). Nonetheless, a positive *EP* is maintained for price fluctuations within 10% of the base price.

Theoretically, the supply of the net heat generated to heat networks would represent an opportunity to further reduce the biorefinery's carbon emissions through application of carbon credits. However, the Derbyshire coffee factory considered in this study is one of more than 20 Nestlé coffee factories worldwide currently incinerating the SCG it produces to meet the factory's heat energy requirements ("Grounds for sustainability: coffee for energy, fuel and a cleaner world," 2013). Future studies on the valorisation of SCG from instant coffee factories must thus account for the economic and environmental impact of diverting SCG to a biorefinery and away from combustion to generate the heat requirements of the factory. Including this in the analysis would likely have negative implications on both the economics and emissions of the SCG biorefinery. However, the

biorefinery strategy could still represent a more profitable method of utilising SCG waste than combustion. As size was found to be an important factor affecting the economic performance and risk of a SCG biorefinery, different coffee factory sizes should be explored in these studies.

Additionally, the environmental evaluations of this study only considered GHG emissions. The environmental performances of the scenarios may differ upon assessment of other categories such as acidification potential and human toxicity potential. Other environmental impact categories should also be evaluated in future studies for a more holistic view of SCG biorefinery environmental performance.

Oil extraction and PHB production were identified as the processes with the largest costs in Scenarios A and D (see Figure D.3 of Appendix D). *n*-hexane and cellulase represent 25% and 17% of the total annual costs of Scenarios A and D, respectively. Thus, further studies on biodiesel and PHB production from SCG should aim to reduce usage of *n*-hexane and cellulase to maximise potential cost reductions. The technologies used in Scenario C must also be scaled to pilot plant levels to verify technical feasibility of the SCG biorefinery strategy. The accuracy of this study's results depends heavily on the financial investments and engineering capability required to scale these processes up economically.

5 Conclusions

This study investigates the future prospects of SCG biorefineries by assessing four SCG biorefinery scenarios in terms of their economic and environmental performances. The parameters altered between scenarios include biorefinery size, design configuration and location relative to the SCG source. SCG was either obtained from London coffee establishments or a coffee factory in Derbyshire. Two biorefinery configurations were used, with one producing biodiesel and electricity (Configuration I) and the other biodiesel with a range of high-value chemicals (Configuration II).

Overall, the results of this study indicate that future SCG biorefineries are likely to be of large scale and located on the site of an instant coffee factory. Heightened growth in demand for advanced biofuels coupled with pressures to reduce factory emissions mean that the waste-to-fuel biorefinery pathway could be regarded as an economically and environmentally attractive additional value chain for coffee factories. Provided that the relevant technologies can be successfully scaled up, production of multiple high-value chemicals is likely to be incorporated into SCG biorefineries due to attractive economic returns. Implementation of sustainable on-site energy generation will be crucial to minimise the high GHG emissions of the plant. Finally, SCG biorefineries have the potential to meet growing biodiesel demand, with similar production costs and lower GHG emissions when compared to conventional biodiesel.

Acknowledgement

This work was supported by the UKRI Natural Environment Research Council (NE/R012938/1) through the UKRI/NERC Industrial Innovation Fellowship Programme.

References

Abdelaziz, O.Y., Al-Rabiah, A.A., El-Halwagi, M.M., Hulteberg, C.P., 2020. Conceptual design of a kraft lignin biorefinery for the production of valuable chemicals via oxidative depolymerization. ACS Sustainable Chemistry and Engineering. 8, 8823–8829. https://doi.org/10.1021/acssuschemeng.0c02945

Abdelaziz, O.Y., Ravi, K., Mittermeier, F., Meier, S., Riisager, A., Lidén, G., Hulteberg, C.P., 2019. Oxidative Depolymerization of Kraft Lignin for Microbial Conversion. ACS Sustainable Chemistry and Engineering. 7, 11640–11652. https://doi.org/10.1021/acssuschemeng.9b01605

Al-Hamamre, Z., Foerster, S., Hartmann, F., Kröger, M., Kaltschmitt, M., 2012. Oil extracted from spent coffee grounds as a renewable source for fatty acid methyl ester manufacturing. Fuel. 96, 70–76. https://doi.org/10.1016/j.fuel.2012.01.023

Allesina, G., Pedrazzi, S., Allegretti, F., Tartarini, P., 2017. Spent coffee grounds as heat source for coffee roasting plants: Experimental validation and case study. Applied Thermal Engineering. 126, 730-736. https://doi.org/10.1016/j.applthermaleng.2017.07.202

Bio-bean, 2021. Coffee logs. https://www.bio-bean.com/coffee-logs/ (accessed 17 May 2021)

Caetano, N.S., Silva, V.F.M., Melo, A.C., Martins, A.A., Mata, T.M., 2014. Spent coffee grounds for biodiesel production and other applications. Clean Technologies and Environmental Policy.

16, 1423–1430. https://doi.org/https://doi.org/10.1007/s10098-014-0773-0
Davis, R., Tao, L., Tan, E.C.D., Biddy, M.J., Beckham, G.T., Scarlata, C., Jacobson, J., Cafferty, K., Ross, J., Lukas, J., Knorr, D., Schoen, P., 2013. Process design and economics for the conversion of lignocellulosic biomass to hydrocarbons: dilute-acid and enzymatic deconstruction of biomass to sugars and biological conversion of sugars to hydrocarbons. www.nrel.gov/publications (accessed 7 May 2021).
Department for Environment, Food and Rural Affairs (DEFRA), the Department of Agriculture, Environment and Rural Affairs (DAERA), the Welsh Government and the Scottish Government, 2020. Circular economy package policy statement. https://www.gov.uk/government/publications/circular-economy-package-policy-statement/circular-economy-package-policy-statement (accessed 18 May 2021).
Efthymiopoulos, I., Hellier, P., Ladommatos, N., Russo-Profili, A., Eveleigh, A., Aliev, A., Kay, A., Mills-Lamptey, B., 2018. Influence of solvent selection and extraction temperature on yield and composition of lipids extracted from spent coffee grounds. Industrial Crops and Products. 119, 49–56. https://doi.org/10.1016/j.indcrop.2018.04.008
Fujita, I., Wada, K., 2008. A process for producing succinic acid. WO2008010373. https://patentscope.wipo.int/search/en/detail.jsf?docId=WO2008010373&tab=PCTBIBLIO (accessed 14 April 2021)
Giller, C., Malkani, B., Parasar, J., 2017. Coffee to Biofuels. Senior Design Reports (CBE). 94. University of Pennsylvania. https://repository.upenn.edu/cbe_sdr/94/ (accessed 11 April 2021).
Gómez-Ríos, D., Navarro, G., Monsalve, P., Barrera-Zapata, R., Ríos-Estepa, R., 2019. Aspen plus simulation strategies applied to the study of chitin ioextraction from shrimp waste. Food Technology and Biotechnology.. 57, 238–248. https://doi.org/10.17113/ftb.57.02.19.6003
Guardian, 2013. Grounds for sustainability: coffee for energy, fuel and a cleaner world. https://www.theguardian.com/sustainable-business/grounds-sustainability-coffee-energy-fuel-pollution (accessed 16 May 2021).
Hochegger, M., Cottyn-Boitte, B., Cézard, L., Schober, S., Mittelbach, M., Li, H., 2019. Influence of Ethanol Organosolv Pulping Conditions on Physicochemical Lignin Properties of European Larch. International Journal of Chemical Engineering. 2019, 1734507. https://doi.org/10.1155/2019/1734507
Humbird, D., Davis, R., Tao, L., Kinchin, C., Hsu, D., Aden, A., Schoen, P., Lukas, J., Olthof, B., Worley, M., Sexton, D., Dudgeon, D., 2011. Process Design and Economics for Biochemical Conversion of Lignocellulosic Biomass to Ethanol: Dilute-Acid Pretreatment and Enzymatic Hydrolysis of Corn Stover. https://doi.org/10.2172/1013269
IEA Bioenergy, 2021. Fossil and biogenic carbon emissions. https://www.ieabioenergy.com/iea-publications/faq/woodybiomass/biogenic-co2/ (accessed 14 May 2021).
International Energy Agency, 2012. World Energy Outlook 2012. https://www.iea.org/reports/world-energy-outlook-2012 (accessed 7 May 2021).
International Organization for Standardization, 2018. ISO 14067:2018, Carbon footprint of products. https://www.iso.org/obp/ui/#iso:std:iso:14067:ed-1:v1:en (accessed 15 May 2021).
Kang, S.B., Oh, H.Y., Kim, J.J., Choi, K.S., 2017. Characteristics of spent coffee ground as a fuel and combustion test in a small boiler (6.5 kW). Renewable Energy. 113, 1208-1214. https://doi.org/10.1016/j.renene.2017.06.092
Karmee, S.K., 2018. A spent coffee grounds based biorefinery for the production of biofuels, biopolymers, antioxidants and biocomposites. Waste Management. 72, 240-254. https://doi.org/10.1016/j.wasman.2017.10.042
Kondamudi, N., Mohapatra, S.K., Misra, M., 2008. Spent Coffee Grounds as a Versatile Source of Green Energy. Journal of Agricultural and Food Chemistry. 56, 11757–11760. https://doi.org/10.1021/jf802487s
Kookos, I. K., 2018. Technoeconomic and environmental assessment of a process for biodiesel production from spent coffee grounds (SCGs). Resources, Conservation and Recycling. 134, 156–164. https://doi.org/10.1016/j.resconrec.2018.02.002

Kourmentza, C., Economou, C.N., Tsafrakidou, P., Kornaros, M., 2018. Spent coffee grounds make much more than waste: Exploring recent advances and future exploitation strategies for the valorization of an emerging food waste stream. Journal of Cleaner Production. 172, 980–992. https://doi.org/10.1016/j.jclepro.2017.10.088

Lee, M., Yang, M., Choi, S., Shin, J., Park, C., Cho, S.K., Kim, Y.M., 2019. Sequential production of lignin, fatty acid methyl esters and biogas from spent coffee grounds via an integrated physicochemical and biological process. Energies. 12, 2360. https://doi.org/10.3390/en12122360

Li, Q., Xing, J., Li, W., Liu, Q., Su, Z., 2009. Separation of Succinic Acid from Fermentation Broth Using Weak Alkaline Anion Exchange Adsorbents. Industrial and Engineering Chemistry Research. 48, 3595–3599. https://doi.org/10.1021/ie801304k

Limousy, L., Jeguirim, M., Dutournié, P., Kraiem, N., Lajili, M., Said, R., 2012. Gaseous products and particulate matter emissions of biomass residential boiler fired with spent coffee grounds pellets. Fuel. 107, 323-329. https://doi.org/10.1016/j.fuel.2012.10.019

Martinez-Saez, N., García, A.T., Pérez, I.D., Rebollo-Hernanz, M., Mesías, M., Morales, F.J., Martín-Cabrejas, M.A., del Castillo, M.D., 2017. Use of spent coffee grounds as food ingredient in bakery products. Food Chemistry. 216, 114–122. https://doi.org/10.1016/j.foodchem.2016.07.173

Massaya, J., Prates Pereira, A., Mills-Lamptey, B., Benjamin, J., Chuck, C.J., 2019. Conceptualization of a spent coffee grounds biorefinery: A review of existing valorisation approaches. Food and Bioproducts Processing. 118, 149–166. https://doi.org/10.1016/j.fbp.2019.08.010

Mata, T.M., Martins, A.A., Caetano, N.S., 2018. Bio-refinery approach for spent coffee grounds valorization. Bioresource Technology. https://doi.org/10.1016/j.biortech.2017.09.106

Mayson, S., Williams, I.D., 2021. Applying a circular economy approach to valorize spent coffee grounds. Resources, Conservation and Recycling. 172, 105659. https://doi.org/10.1016/j.resconrec.2021.105659

McNutt, J., He, Q., 2018. Spent coffee grounds: A review on current utilization. Journal of Industrial and Engineering Chemistry. 71, 78-88. https://doi.org/10.1016/j.jiec.2018.11.054

Mussatto, S.I., Carneiro, L.M., Silva, J.P.A., Roberto, I.C., Teixeira, J.A., 2011. A study on chemical constituents and sugars extraction from spent coffee grounds. Carbohydrate Polymers. 83, 368–374. https://doi.org/10.1016/j.carbpol.2010.07.063

Najdanovic-Visak, V., Lee, F.Y.L., Tavares, M.T., Armstrong, A., 2017. Kinetics of extraction and in situ transesterification of oils from spent coffee grounds. Journal of Environmental Chemical Engingeering. 5, 2611–2616. https://doi.org/10.1016/j.jece.2017.04.041

Ng, D.K.S., Ng, K.S., Ng, R.T.L., 2017. Integrated biorefineries, in: Abraham, M.A. (Eds.), Encyclopedia of Sustainable Technologies. Elsevier, Oxford, pp. 299-314.

Ng, K.S., Martinez-Hernandez, E., 2020. Techno-economic assessment of an integrated bio-oil steam reforming and hydrodeoxygenation system for polygeneration of hydrogen, chemicals, and combined heat and power production, in: Ren, J., Wang, Y., He, C. (Eds), Towards Sustainable Chemical Processes. Elsevier, Oxford, pp. 69-98

Ng, K.S., Yang, A., Yakovleva, N., 2019. Sustainable waste management through synergistic utilisation of commercial and domestic organic waste for efficient resource recovery and valorisation in the UK. Journal of Cleaner Production. 227, 248–262. https://doi.org/10.1016/j.jclepro.2019.04.136

Ng, K.S., Zhang, N., Sadhukhan, J., 2013. Techno-economic analysis of polygeneration systems with carbon capture and storage and CO2 reuse. Chemical Engineering Journal. 219, 96–108. https://doi.org/10.1016/j.cej.2012.12.082

Nieder-Heitmann, M., Haigh, K., Görgens, J.F., 2019. Process design and economic evaluation of integrated, multi-product biorefineries for the co-production of bio-energy, succinic acid, and

polyhydroxybutyrate (PHB) from sugarcane bagasse and trash lignocelluloses. Biofuels, Bioproducts and Biorefining 13, 599–617. https://doi.org/10.1002/bbb.1972
Obruca, S., Benesova, P., Kucera, D., Petrik, S., Marova, I., 2015. Biotechnological conversion of spent coffee grounds into polyhydroxyalkanoates and carotenoids. New Biotechnolgy. 32, 569–574. https://doi.org/10.1016/j.nbt.2015.02.008
Panusa, A., Zuorro, A., Lavecchia, R., Marrosu, G., Petrucci, R., 2013. Recovery of natural antioxidants from spent coffee grounds. Journal of Agricultural and Food Chemistry. 61, 4162–4168. https://doi.org/10.1021/jf4005719
Park, J., Kim, B., Lee, J.W., 2016. In-situ transesterification of wet spent coffee grounds for sustainable biodiesel production. Bioresource Technology. 221, 55–60. https://doi.org/10.1016/j.biortech.2016.09.001
Phillips, S., Flach, B., Lieberz, S., Bolla, S., 2019. USDA EU Biofuels Annual. https://www.fas.usda.gov/data/eu-28-biofuels-annual-1 (accessed 15 March 2021).
Recycling Magazine, 2019. Reducing coffee waste. https://www.recycling-magazine.com/2019/10/01/reducing-coffee-waste/ (accessed 21 April 2021).
Rivera, X.C.S., Gallego-Schmid, A., Najdanovic-Visak, V., Azapagic, A., 2020. Life cycle environmental sustainability of valorisation routes for spent coffee grounds: From waste to resources. Resources, Conservation and Recycling. 157, 104751. https://doi.org/10.1016/j.resconrec.2020.104751
Sadhukhan, J., Ng, K.S., Hernandez, E.M., 2014. Biorefineries and chemical processes : design, integration and sustainability analysis, Ebook central. John Wiley & Sons Ltd, Chichester.
Saratale, G., Bhosale, R., Shobana, S., Rajesh Banu, J., Pugazhendhi, A., Mahmoud, E., Sirohi, R., Kant Bhatia, S., Atabani, A.E., Mulone, V., Yoon, J.-J., Shin, H.S., Kumar, G., 2020. A review on valorization of spent coffee grounds (SCG) towards biopolymers and biocatalysts production. Bioresource Technology. 314, 123800. https://doi.org/10.1016/j.biortech.2020.123800
Somnuk, K., Eawlex, P., Prateepchaikul, G., 2017. Optimization of coffee oil extraction from spent coffee grounds using four solvents and prototype-scale extraction using circulation process. Agriculture and Natural Resources. 51, 181–189. https://doi.org/10.1016/j.anres.2017.01.003
Thoppil, Y., Zein, S.H., 2021. Techno-economic analysis and feasibility of industrial-scale biodiesel production from spent coffee grounds. Journal of Cleaner Production. 307, 127113. https://doi.org/10.1016/j.jclepro.2021.127113
Trejo-Zárraga, F., Hernández-Loyo, F. de J., Chavarría-Hernández, J.C., Sotelo-Boyás, R., 2018. Kinetics of Transesterification Processes for Biodiesel Production, in: Biofuels - State of Development. IntechOpen, pp. 149–179. https://doi.org/10.5772/intechopen.75927
Tsoutsos, T., Tournaki, S., Gkouskos, Z., Paraíba, O., Giglio, F., García, P.Q., Braga, J., Adrianos, H., Filice, M., 2019. Quality characteristics of biodiesel produced from used cooking oil in Southern Europe. ChemEngineering 3, 1–13. https://doi.org/10.3390/chemengineering3010019
Tuntiwiwattanapun, N., Monono, E., Wiesenborn, D., Tongcumpou, C., 2017. In-situ transesterification process for biodiesel production using spent coffee grounds from the instant coffee industry. Industrial Crops and Products. 102, 23–31. https://doi.org/10.1016/j.indcrop.2017.03.019
van Ree, R., de Jong, E., Kwant, K., 2012. Bio-based chemicals: value added products from biorefineries. https://www.ieabioenergy.com/blog/publications/bio-based-chemicals-value-added-products-from-biorefineries/ (accessed 7 May 2021).
Zetterholm, J., Bryngemark, E., Ahlström, J., Söderholm, P., Harvey, S., Wetterlund, E., 2020. Economic Evaluation of Large-Scale Biorefinery Deployment: A Framework Integrating Dynamic Biomass Market and Techno-Economic Models. Sustainability. 12, 7126. https://doi.org/10.3390/su12177126